



## Tohdite recovery from water by fluidized-bed homogeneous granulation process

Anabella C. Vilando<sup>a,b</sup>, Alvin R. Caparanga<sup>b</sup>, Yao-Hui Huang<sup>c</sup>, Ming-Chun Lu<sup>d,\*</sup>

<sup>a</sup>Department of Chemical Engineering, College of Engineering, Adamson University, Ermita, Manila, Philippines, emails: acv\_rev@yahoo.com.ph, anabella.vilando@adamson.edu.ph

<sup>b</sup>School of Chemical Engineering and Chemistry, Mapúa University, Intramuros, Manila, Philippines, emails: alvinrcaparanga@gmail.com, arcaparanga@mapua.edu.ph (A.R. Caparanga)

<sup>c</sup>Department of Chemical Engineering, National Cheng Kung University, Tainan 701, Taiwan, email: yhhuang@mail.ncku.edu.tw

<sup>d</sup>Department of Environmental Resources Management, Chia Nan University of Pharmacy and Science, Tainan 71710, Taiwan, email: mmclu@mail.cnu.edu.tw

Received 20 January 2017; Accepted 3 October 2017

### ABSTRACT

Fluidized-bed homogeneous granulation process (FBHGP) is an advanced process that can remove heavy metals in wastewaters by forming densified granules without using seed material. This investigation studies the aluminum recovery from water by FBHGP. The effluent pH ( $\text{pH}_e$ ) was an essential factor in determining the efficacy of FBHGP in terms of Al removal (%) and granulation ratio (GR, %). The Al removal % that was achieved by the growth of aluminum oxide hydrate nuclei at  $300 \text{ mg}\cdot\text{L}^{-1}$  with an influent molar ratio of  $[\text{H}_2\text{O}_2]_{\text{in}}/[\text{Al}^{3+}]_{\text{in}} = 2.50$  was 99.12% at  $\text{pH}_e = 9.0 \pm 0.2$ . However, the GR of 96.47% that transformed the crystalline phase of granular pellets from aluminum hydroxide to aluminum oxide hydrate ( $\text{Al}_{10}\text{O}_{15}\cdot\text{H}_2\text{O}$ -Tohdite) was confirmed by the X-ray diffraction analysis. An effective FBHG process ran under a supersaturation was close to the metastable region, as discussed by the evaluations of hydraulic conditions and supersolubility activities in the effluent. To conclude, a practical way of recovering aluminum from aqueous solution into a granule form and non-toxic compound of aluminum oxide hydrate was done.

*Keywords:* Tohdite; Fluidized-bed; Granulation; Supersaturation

### 1. Introduction

The Earth's surface is composed of about 8% aluminum, which occurs naturally in bauxite rocks, silicates and cryolite. Occurrence of aluminum in drinking water and food-stuffs comes from different uses [1]. According to reports, regions exposed to acid precipitation have water systems with aluminum concentration 10 times those of fresh water systems [2]. The fatal concentration of dissolved aluminum from water affected by acid mine drainage is about  $90 \text{ mg}\cdot\text{L}^{-1}$  [3,4]. The occurrence of aluminum in drinking water has given considerations on possible effects on human health,

that is, Alzheimer's disease and dialysis encephalopathy [3]. However, alumina is widely used in fused form (alundum or aloxite) in different applications. More than 90% of the 45 million metric tons of annual world production of alumina is used in the manufacture of aluminum metal. Specialty aluminum oxides are used in ceramics, refractories, chemical industries, catalyst, fillers and glass industry, and polishing and abrasive applications. Huge capacities are used in the manufacture of coating titanium pigments, zeolites, and as smoke suppressant/fire retardant [5].

Recognized alum coagulants such as aluminum sulfate,  $\text{Al}_2(\text{SO}_4)_3$ , or polyaluminum chloride, are used to improve

\* Corresponding author.

the removal of colloidal, particulate matters, and dissolved substances in the treatment of drinking water. More aluminum is present in treated water due to regular use of alum as coagulants [6]. Dissolved aluminum is the major contaminant in wastewaters of aluminum finishing processes that require successive wastewater treatment methods, such as neutralization, clarification, and dewatering.

The most commonly used technique in heavy metal recovery is chemical precipitation due to its efficiency and low operation cost. However, it gathers large amount of sludge that has high water content, which is a major concern [7–9]. Fluidized-bed homogeneous granulation process (FBHGP) is a better method because it uses small amount of chemicals and produces an extremely low moisture content granules [10,11]. Fluidized-bed reactors (FBRs) have been used widely to treat wastewaters having heavy metals (Cu, Zn, Ni, As) and inorganic acids (boric, phosphoric) [12–16]. The FBHGP can be an alternative method in the recovery and treatment of aluminum from aluminum finishing processes. It is an advanced process that can produce granules without the presence of a seed material. By adjusting the reactor conditions, granulation happened inside the reactor. FBHGP has presented greater leads than the other treatment methods in terms of economics, effectiveness, space availability, accumulation of slurry, and can produce a low water content granule products [17].

Crystallization can be achieved by controlling the hydraulic parameters that distribute sufficient collisions for gathering fine nuclei in FBR [18]. The driving force of crystallization that leads to supersaturation is governed by solubility product constant ( $K_{sp}$ ) [19,20]. The concentration, pH, and pollutant loadings per unit area per hour control the supersaturation of the water systems in FBC that affects the metal removal and crystallization efficiency [21]. The nucleation in the FBR can be measured with the hydraulic parameters at the metastable region forming heavy crystals rather than a soft high moisture sludge [22].

This study deals with the recovery of aluminum as aluminum oxide hydrate ( $Al_10O_{15} \cdot xH_2O$  or tohdite) via hydrogen peroxide ( $H_2O_2$ ) route by FBHGP. The best operating parameters – influent aluminum concentration, effluent pH ( $pH_e$ ), and molar ratio (MR) of precipitant to metal  $[H_2O_2]_{in}/[Al^{3+}]_{in}$  – were determined. The dependence of  $pH_e$  on the total  $[Al^{3+}]_t$  and soluble  $[Al^{3+}]_s$  aluminum concentrations in the effluent were also determined. The quality of effluent was analyzed by inductively coupled plasma-optical emission spectrometer (ICP-OES). The formed granules were characterized using scanning electron microscope (SEM), energy dispersive X-ray spectroscopy (EDS), and X-ray diffraction (XRD).

## 2. Materials and methods

### 2.1. Chemicals

The reagents used were of analytical grade and were used without further purification.  $AlCl_3 \cdot 6H_2O$  (97%, Katayama Chemicals, Co. Ltd., Japan) was used to prepare the synthetic aluminum wastewater at specified concentrations. The precipitant used was sodium carbonate ( $Na_2CO_3$ , AppliChem Panreac ITW Companies, Germany) and hydrogen peroxide ( $H_2O_2$ , 35%, Chang Chung Petrochemicals, Ltd., Taiwan).

To adjust the pH of the precipitant, sodium hydroxide (NaOH, 99.38%, Choneye Pure Chemicals) and hydrochloric acid (HCl, 37%, Merck, Germany) were used. The water used for preparing all the solutions was deionized using a laboratory grade RO-ultrapure water system (resistance > 18.2  $\Omega$ ).

### 2.2. Fluidized-bed apparatus

The reactor, having a total volume of 550 mL, is made of a cylindrical Pyrex glass column (Fig. 1). The upper column has a diameter of 4.0 cm and a height of 20 cm; the lower column has 2.0 cm (diameter) and 80 cm (height). There are three inlets at the bottom of the reactor that are connected to a peristaltic pump to control the flows of the influent Al wastewater ( $Q_{Al}$ ), the precipitant ( $Q_{H_2O_2+Na_2CO_3}$ ), and the reflux flow ( $Q_r$ ). To uniformly distribute the hydraulic loading and to support the granulation bed, glass beads were packed with a height of 4.0 cm. The important parameters and nomenclature are tabulated in Table 1.

### 2.3. Experimental procedure and analytical techniques

FBHGP was performed by adjusting the flow rates of the influent metal ( $Q_{Al}$ ), the precipitant ( $Q_{H_2O_2+Na_2CO_3}$ ) and the reflux flows ( $Q_r$ ). The mixing of 100 to 400  $mg \cdot L^{-1} [Al^{3+}]_{in}$  and  $[H_2O_2]_{in}$  yields a MR of  $[H_2O_2]_{in}/[Al^{3+}]_{in} = 1.5, 2.0,$  and 2.5 with effluent pH of 7.0, 8.0, 9.0, 9.5, and 10.0. At the start, the solution was turbid and nucleation occurred. The nuclei that formed on top of the glass beads moved upward with the flow that formed cloudy agglomerates. The collision of the grown particles made them to slow down and became fluidized in the reaction region. Small particles were visible in 10–14 d. Successively, the consistent run of Al removal started with

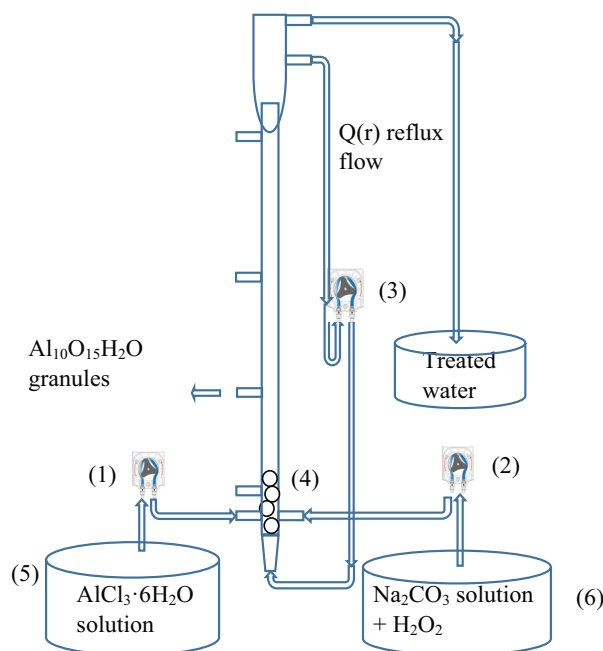


Fig. 1. Fluidized-bed reactor set up. (1) Peristaltic pump for synthetic aluminum wastewater; (2) peristaltic pump for the precipitant; (3) peristaltic pump for the reflux; (4) glass beads; (5) synthetic aluminum wastewater tank; (6) precipitant tank.

Table 1  
Nomenclature definition of hydraulic parameters in FBHGP

Symbol	Definition	Remarks
$Q_{[Al^{3+}]}$	Influent flow rate of aluminum ion, mL·min <sup>-1</sup>	
$Q_{H_2O_2+Na_2CO_3}$	Influent flow rate of precipitant, mL·min <sup>-1</sup>	
$Q_t$	Total influent flow rate, mL·min <sup>-1</sup>	$Q_{H_2O_2+Na_2CO_3}$
$Q_r$	Reflux flow rate, mL·min <sup>-1</sup>	
$[Al^{3+}]_{in}$	Inlet concentration of aluminum salt, mM	
$[Al^{3+}]_t$	Effluent total aluminum concentration, mM	
$[Al^{3+}]_s$	Effluent soluble aluminum concentration, mM	
$[Na_2CO_3]$	Inlet concentration of sodium carbonate with H <sub>2</sub> O <sub>2</sub> , mM	
$[H_2O_2]_{in}/[Al^{3+}]_{in}$	Inlet molar ratio	
$A_{low}$	Internal cross-section area of reaction region, m <sup>2</sup>	
$A_{up}$	Internal cross-section area of effluent region, m <sup>2</sup>	
$U$	Upflow velocity (hydraulic loading), m·h <sup>-1</sup>	$(Q_t + Q_r)/A_{low}$
$U_{out}$	Effluent velocity, m·h <sup>-1</sup>	$Q_t/A_{up}$
$L$	Cross-section loading, kg·m <sup>-2</sup> ·h <sup>-1</sup>	$Q_{Al}[Al^{3+}]_{in}/A_{low}$
$V_T$	Total volume of reaction solution in reactor, mL	
HRT	Hydraulic retention time, min	$V_T/Q_t$
pH <sub>e</sub>	Effluent Ph	

the progressive polymerization of Al(OH)<sub>3</sub> particles. The preferred hydraulic retention time was between 9.32 and 32.59 min ( $Q_t = 44\text{--}60\text{ mL}\cdot\text{min}^{-1}$ ) with cross-section loading ( $L$ ) of 1.224–1.528 kg·m<sup>-2</sup>·h<sup>-1</sup>. The water chemistry and measurement of effluent pH as it reached equilibrium had at least nine times HRT (~1.37 h) after adjusting the parameters of the whole system.

For effluent sampling, 5 mL was taken twice from the effluent region. One sample was filtered with 0.45 μm (GHP membrane, Pall), the other one was not. Both samples were treated with 0.1 M HCl to decrease the supersaturation. The soluble  $[Al^{3+}]_s$  concentration is the Al concentration in the filtrates and the total  $[Al^{3+}]_t$  concentration is the Al concentration in acidic digestion. The effectiveness of the FBHGP was evaluated by Al removal (%) and GR (%).

$$\text{Al removal (\%)} = \left( 1 - \frac{[Al^{3+}]_s \cdot Q_t}{[[Al^{3+}]_{in} \cdot Q_{Al}]} \right) \times 100 \quad (1)$$

$$\text{GR (\%)} = \left( 1 - \frac{[Al^{3+}]_t \cdot Q_t}{[[Al^{3+}]_{in} \cdot Q_t]} \right) \times 100 \quad (2)$$

Al removal (%) determines the residual Al in discharges of the FBR, while GR (%) is the capability of the FBR conditions to recover Al in granule form with low water content rather than a soft sludge.

The effluent concentrations of  $[Al^{3+}]_s$  and  $[Al^{3+}]_t$  were analyzed using ICP-OES (ULTIMA 2000, HORIBA Ltd., Japan). The morphology of the granules was analyzed using SEM (JSM-6700F, JEOL Ltd., Japan), for the elemental distribution using (EDS, LINKS AN10000/85S), and the crystallographic structure was determined using XRD (DX III, Rigaku Co., Japan) patterns with a CuKα radiation source

( $\lambda = 1.5406 \text{ \AA}$ ), and a scanning rate of 0.06° s<sup>-1</sup> in the incidence angle of 10–80 (2θ).

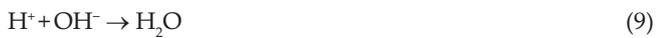
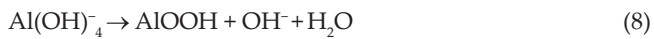
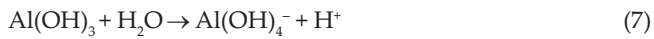
### 3. Results and discussions

#### 3.1. Formation of aluminum complexes

FBHGP was operated continuously at normal room temperature. To determine the effects of parameters on the metal removal and granulation, varying one parameter and the other two parameters were held constant. The best operating parameters were the influent  $[Al^{3+}]_{in}$  concentration of 300 mg·L<sup>-1</sup> ( $U = 24.35\text{ m}\cdot\text{h}^{-1}$ ), MR of  $[H_2O_2]_{in}/[Al^{3+}]_{in}$  of 2.5, and effluent pH of 9.0 ± 0.2.

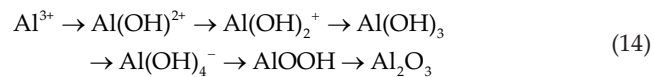
Aluminum shows complexity in dilute solutions. Reactions that involve  $[Al^{3+}]$  and  $[OH^-]$  are slow at room temperature. Metastable solid species form and equilibrium conditions are hard to achieve even at long period of reactions. Aging the solution for 3 years to polymerize the Al species results in the formation of tiny crystals in alkaline solution that are comparable to bayerite of 0.001 mm crystal diameter. As pH is increased, the hydroxyl–aluminum complexes form. Increase in Al ions involved in the polynuclear complexes, bigger structural units, become colloidal and form a suspension of compact crystal particles that turn into a solid [23]. The complete chemical synthesis route for the granulation of Al<sub>2</sub>O<sub>3</sub> and its byproducts were shown in Eqs. (3)–(13). The use of H<sub>2</sub>O<sub>2</sub> in the solution shortens the aging process. The base-catalyzed decomposition reaction that is in equilibrium and interrelated to the ionization process of H<sub>2</sub>O<sub>2</sub> has been shown in Eqs. (9)–(11) [24]:





The pH of the solution is reduced to an acceptable value of 12 for the advanced polymerization of hydroxo-aqua  $\text{Al}(\text{OH})_4^-$  to insoluble permeable boehmite [25,26]. The summary of the precipitation process is stated in Eq. (8).

When the alkalinity of the solution is too strong at high MR, only small amount of free  $\text{OH}^-$  is neutralized and the required precipitation reaction cannot proceed. The solution via  $\text{H}_2\text{O}_2$  route can be extended to basic solutions at low MR of  $\text{H}_2\text{O}_2$  to  $\text{Al}_2\text{O}_3$  [27]. Boehmite is the stable  $\text{AlO}(\text{OH})$  polymorphs at low temperature and pressure. The conversion of  $\text{Al}(\text{OH})_3$  to  $\text{AlOOH}$  is a function of water, also the conversion of diaspre ( $\alpha\text{-AlOOH}$ ) to corundum ( $\alpha\text{-Al}_2\text{O}_3$ ) is due to the decrease of water activity towards equilibrium at low temperature [28]. The conversion path is as follows [29]:



### 3.2. Effect of $\text{pH}_e$ on Al removal and granulation

Inflow rates of the Al and  $\text{Na}_2\text{CO}_3$  with  $\text{H}_2\text{O}_2$  were controlled to achieve the desired pH of the effluent. The reflux flow rate ( $Q_r$ ) was controlled at  $90 \text{ mL}\cdot\text{min}^{-1}$ . The influent concentrations of  $[\text{Al}^{3+}]$  were  $100\text{--}400 \text{ mg}\cdot\text{L}^{-1}$  and the MR of  $[\text{H}_2\text{O}_2]_{\text{in}}/[\text{Al}^{3+}]_{\text{in}}$  were 1.5, 2.0, and 2.5. Increasing the concentration of the precipitant ( $\text{Na}_2\text{CO}_3 + \text{H}_2\text{O}_2$ ) increases the pH of the solution. At 1.5 MR of  $[\text{H}_2\text{O}_2]_{\text{in}}/[\text{Al}^{3+}]_{\text{in}}$  and  $267 \text{ mg}\cdot\text{L}^{-1}$  influent Al concentration with hydraulic loading ( $U$ ) of

$27.33 \text{ m}\cdot\text{h}^{-1}$ , the highest Al removal (%) was attained at 96.81% and 98.76% for  $400 \text{ mg}\cdot\text{L}^{-1}$  with hydraulic loading ( $U$ ) of  $27.69 \text{ m}\cdot\text{h}^{-1}$  at effluent pH  $9.5 \pm 0.2$  (Fig. 2(a)). For 2.0 MR of  $[\text{H}_2\text{O}_2]_{\text{in}}/[\text{Al}^{3+}]_{\text{in}}$  at  $100 \text{ mg}\cdot\text{L}^{-1}$  ( $U = 26.74 \text{ m}\cdot\text{h}^{-1}$ ) influent Al concentration, increasing the effluent pH from 7 to 9, tend

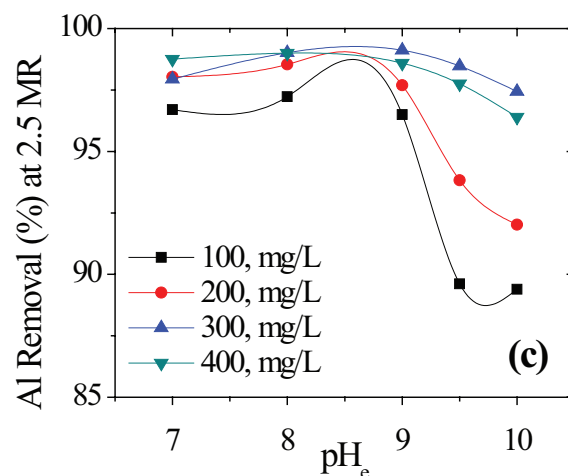
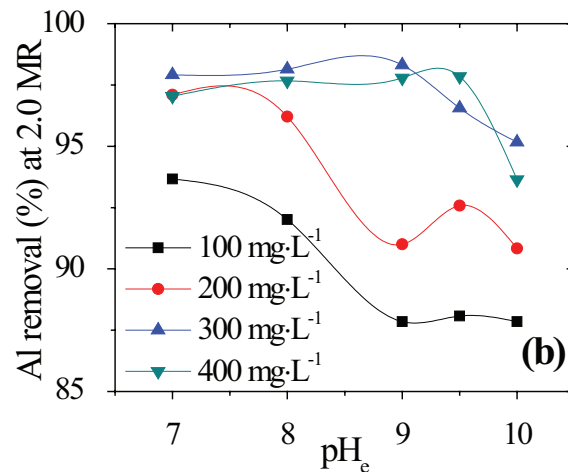
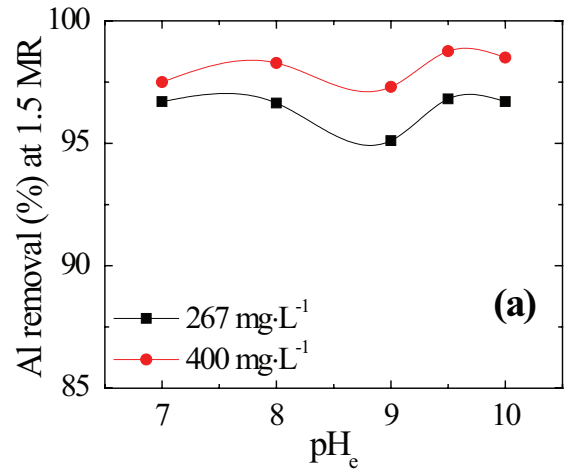


Fig. 2. Aluminum removal (%) at (a) 1.5 (b) 2.0 and (c) 2.5 MR of  $[\text{H}_2\text{O}_2]_{\text{in}}/[\text{Al}^{3+}]_{\text{in}}$  at different pHs of effluent.

to decrease the Al removal (%) of 93.67 to 87.85% and for 200 mg·L<sup>-1</sup> ( $U = 28.46 \text{ m}\cdot\text{h}^{-1}$ ), the Al removal (%) also decreased from 97.10% to 91.00%. Whereas at 300 mg·L<sup>-1</sup> influent Al concentration ( $U = 27.88 \text{ m}\cdot\text{h}^{-1}$ ), the highest Al removal (%) of 98.31% was achieved at effluent pH of  $9 \pm 0.2$ . At 400 mg·L<sup>-1</sup> ( $U = 26.74 \text{ m}\cdot\text{h}^{-1}$ ) the highest Al removal (%) of 97.04% was achieved at effluent pH of 9.5 (Fig. 2(b)). Fig. 2(c) shows that at 2.5 MR of  $[\text{H}_2\text{O}_2]_{\text{in}}/[\text{Al}^{3+}]_{\text{in}}$ , the highest Al removal (%) at 100 mg·L<sup>-1</sup> ( $U = 34.57 \text{ m}\cdot\text{h}^{-1}$ ) was 97.23%, 98.54% for 200 mg·L<sup>-1</sup> and 99.00% at 400 mg·L<sup>-1</sup> ( $U = 24.26 \text{ m}\cdot\text{h}^{-1}$ ) were achieved at effluent pH of 8, while at 300 mg·L<sup>-1</sup> with hydraulic loading ( $U$ ) of  $24.35 \text{ m}\cdot\text{h}^{-1}$ , the highest removal was 99.12% at effluent pH of  $9 \pm 0.2$ . Generally, at constant effluent pH of 9 and increasing the Al concentration, tend to increase the Al removal (%), but decreased at 400 mg·L<sup>-1</sup>. The decrease in Al removal (%) at high concentration was due to the formation of different dissolved Al species at MR greater than 1 at increasing pH [30].

Increasing the MR of the precipitant to metal increases the pH of the solutions. An increase in pH of the solution having  $[\text{Al}^{3+}]$  ions, formation of dissolved species involving associated  $[\text{Al}^{3+}]$  and  $[\text{OH}^-]$  occurred. When there is enough supply of  $[\text{OH}^-]$ , a precipitate of  $\text{Al}(\text{OH})_3$  is produced. Further increased in pH, this precipitate is dissolved again in the form of an ion with greater than three hydroxide groups per Al [23]. Further aging of the solution forms the greater solubility of microcrystalline gibbsite which is basically a particle-size result [31]. Fig. 3 shows the GR (%) of the FBR at different pH and MR of  $[\text{H}_2\text{O}_2]_{\text{in}}/[\text{Al}^{3+}]_{\text{in}}$  using 100–400 mg·L<sup>-1</sup> as influent Al concentration. Generally, GR (%) increases as effluent pH is increased. However, at 9.5 effluent pH, the highest GR (%) was achieved at 95.52% for 267 mg·L<sup>-1</sup> and 98.56% for 400 mg·L<sup>-1</sup>, at 1.5 MR of  $[\text{H}_2\text{O}_2]_{\text{in}}/[\text{Al}^{3+}]_{\text{in}}$  (Fig. 3(a)). At MR of 2.0, the highest GR (%) of 94.13% was achieved at 300 mg·L<sup>-1</sup> influent Al concentration with pH of 9.0 (Fig. 3(b)). In this work, at effluent pH of 9.0, 1.5 MR of  $[\text{H}_2\text{O}_2]_{\text{in}}/[\text{Al}^{3+}]_{\text{in}}$  and influent Al concentration of 300 mg·L<sup>-1</sup> showed the highest Al removal (%) that have the greatest GR (%) of 96.47%. Further increase in influent Al concentration to 400 mg·L<sup>-1</sup> tends to decrease the GR (%) to 93.05%.  $\text{Al}(\text{OH})_3$  is an amphoteric hydroxide and it redissolved due to supersaturation at increased pH that favors nucleation and attrition. The surface charge of a particle is generally dependent on the interface between the surface groups and the surface pH. Henceforth, the granulation of aluminum oxide that can be achieved at a specified pH value with the surface charge of the granule is governed by the attraction of each other [32]. The charge on the alumina surface is measured by amphoteric surface ionization reactions. The surface ionization reaction of hydroxyl group of an amphoteric surface and an acid and base at low pH were shown in Eqs. (15) and (16) that results in either a positively charged surface ( $\text{Al}-\text{OH}_2^+$ ) or a negatively charged ( $\text{Al}-\text{O}^-$ ). The point zero charge (PZC) is determined by the values of the surface ionization reaction constants ( $K_{a1}$  and  $K_{a2}$ ) that occurred in the granulation of  $\text{Al}_2\text{O}_3$  [33].

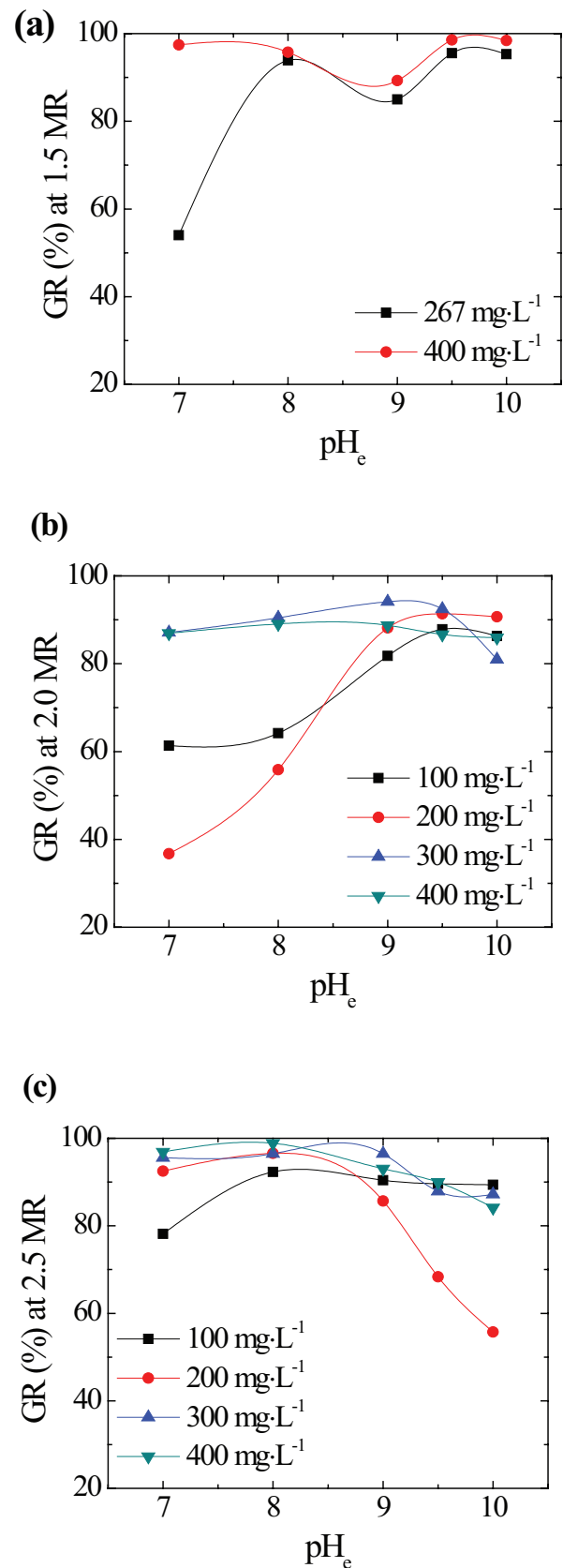
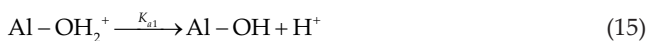


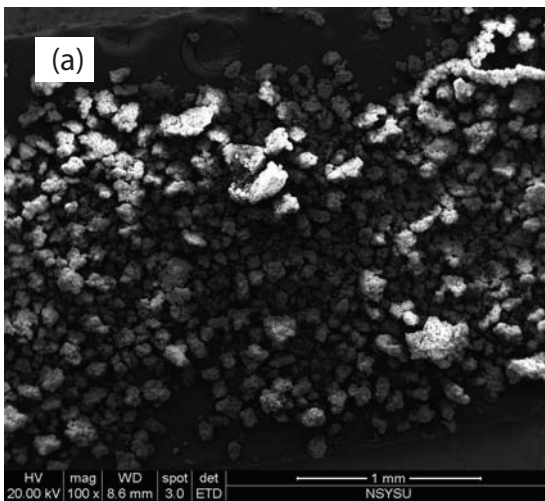
Fig. 3. Granulation ratio (GR) at (a) 1.5 (b) 2.0 and (c) 2.5 MR of  $[\text{H}_2\text{O}_2]_{\text{in}}/[\text{Al}^{3+}]_{\text{in}}$  at different pH of effluent.

The dielectric constants of the solid estimate the PZC of different oxides that include the bond length of the metal hydroxide and bond strength of the Pauling metal-oxygen. An isoelectric potential (IEP) between 8 and 10 for equiaxed aluminum crystals was known. The IEP is known as the pH at zero zeta-potential [34]. Thereby, the amount of the input precipitant should not only be dependable with the stoichiometric relationship of the final granulation product but also it is responsible for the driving force for the granulation (supersaturation) [35].

3.3. Properties of the granules

The SEM microscopic observations of tohdite (Al<sub>10</sub>O<sub>15</sub>H<sub>2</sub>O) granules from FBHGP were shown in Fig. 4(a). The image showed rough flaky grains that are well granulized having a grain diameter of 1.0 mm at 100 magnification. In homogeneous nucleation, colloidal particles are formed initially and continuously for an indefinite period of time. The formed particles are restrained by the impacts that formed bigger particles [21,36,37].

Fig. 4(b) shows the elemental distribution of the formed granules. The formed granules have the composition of aluminum with 11.53% by weight and oxygen of around 88.47% by weight. The excess oxygen in the analysis implies that the granules formed were in hydrated form. Some of the oxygen



(b)

Element	Weight %	Atomic %
O K	88.47	92.83
AlK	11.53	7.17
<b>Total</b>	<b>100.00</b>	<b>100.00</b>

Fig. 4. (a) SEM observation of Al<sub>10</sub>O<sub>15</sub>H<sub>2</sub>O at 100 magnification; (b) EDS ZAP quantification of the granules at 300 mg·L<sup>-1</sup>, MR of H<sub>2</sub>O<sub>2</sub><sub>in</sub>/[Al<sup>3+</sup>]<sub>in</sub> at effluent pH of 9.0.

atoms combined with other cations forming metal oxides that were not quantified in the analysis. The EDS analysis only showed the O and Al atomic ratio and the other components were not accounted in the analysis.

Fig. 5 shows the XRD spectra of the granules formed by FBHGP. The peaks at 36 , 44 , 55 , and 60 represent the spectra of aluminum oxide. Those peaks coincided with the spectra from the XRD patterns of the analyzed granules formed using the FBHGP [29]. Based on the comparison of peaks, the granules formed have the composition as with that of aluminum oxide hydrate (Tohdite-Al<sub>10</sub>O<sub>15</sub>H<sub>2</sub>O).

4. Conclusion

The removal of Al from synthetic wastewater was successfully conducted using FBHGP. Based on the Al removal (%) and GR (%), the best operating parameters were determined. As FBR was continuously operated, stability of aluminum hydroxide was achieved until it was converted to boehmite and eventually to aluminum oxide hydrate in the form of tohdite. At increasing Al concentration from 100 to 300 mg·L<sup>-1</sup> at constant pH, the Al removal (%) and GR (%) is increased, and then decreased at 400 mg·L<sup>-1</sup> due to supersaturation. Since the degree of supersaturation is the driving force in the formation of granules, the best operating condition has a quantitative value of 31.8 by calculating the ratio of the initial concentrations and equilibrium concentrations. At increased pH, the Al removal (%) and GR (%) tend to increase and further increased in pH tend to decrease the metal removal and granulation efficiency. The best operating conditions for the formation of aluminum oxide hydrate were at influent Al concentration of 300 mg·L<sup>-1</sup> with 2.5 MR of [H<sub>2</sub>O<sub>2</sub>]<sub>in</sub>/[Al<sup>3+</sup>]<sub>in</sub> and effluent pH of 9.0 ± 0.2. The highest Al removal (%) at this condition was achieved at 99.12% and the GR (%) was 96.47%. SEM images were measured at 1.0 mm grain diameter at 100 times magnification. EDS results showed that it consists of 11.53% aluminum and 88.47% oxygen. Some of the oxygen atoms were attributed to metal oxides formed that were not quantified in the analysis. The major diffraction peaks showed that the formed granules have the characteristics of aluminum oxide hydrate-tohdite (Al<sub>10</sub>O<sub>15</sub>H<sub>2</sub>O). The FBHGP process that competed under a supersaturation was near to the metastable region, as conferred by the calculations of hydraulic conditions and supersolubility actions in the effluent. To conclude, a useful way of recuperating Al from

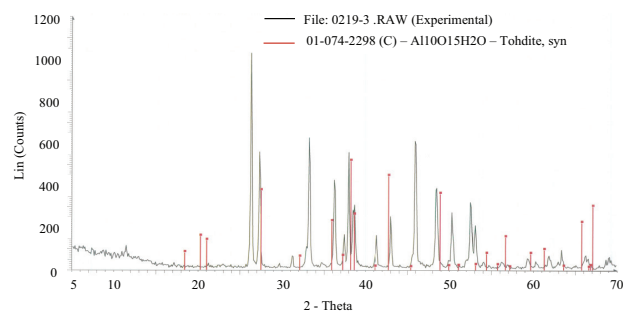


Fig. 5. XRD spectra of the granules at 300 mg·L<sup>-1</sup>, MR of H<sub>2</sub>O<sub>2</sub><sub>in</sub>/[Al<sup>3+</sup>]<sub>in</sub> at effluent pH of 9.0.

aqueous solution into a granule form of innocuous compound of aluminum oxide hydrate was done.

### Acknowledgment

This research project was supported by Ministry of Science and Technology, Taiwan under Contract No. 102-2221-E-041-001-MY3.

### References

- [1] D. Krewski, R.A. Yoke, E. Nieboer, D. Borchelt, J. Cohen, J. Harry, S. Kacew, J. Lindsay, A.M. Mahfouz, V. Virginie Rondeau, Human health risk assessment for aluminium, aluminium oxide, and aluminium hydroxide, *J. Toxicol. Environ. Health B Crit. Rev.*, 10 (2007) 1–269.
- [2] E.T. Gjessing, J. Alexander, B.O. Rosseland, Acidification and Aluminum - Contamination of Drinking Water, Watershed 89: The Future for Water Quality in Europe, 1 (1990) 15–21.
- [3] M.R. Jekel, Aluminum in Water: How It can be Removed? Use of Aluminum Salts in Treatment, *Proc. Int. Water Supply Ass., Copenhagen, Denmark, 1991*, pp. 25–31.
- [4] A.M. Abdullah, Aluminum pollution removal from water using a natural zeolite, *J. Pollut. Effects Control*, 2 (2014) 2–5.
- [5] K. Davis, Material Review: Alumina ( $Al_2O_3$ ), School of Doctoral Studies (European Union), Belgium, 2010.
- [6] P.T. Srinivisan, T. Viraraghavan, K.S. Subramanian, Aluminum in drinking water: an overview, *Water SA.*, 25 (1999) 47–56.
- [7] G. Macchi, M. Pagano, M. Santori, G. Tiravanti, Battery industry wastewater: Pb removal and produced sludge, *Water Res.*, 27 (1993) 1511–1518.
- [8] D. Marani, G. Macchi, M. Pagano, Lead precipitation in the presence of sulphate and carbonate: testing of thermodynamic predictions, *Water Res.*, 29 (1995) 1085–1092.
- [9] G. Macchi, D. Marani, M. Pagano, G. Bagnuolo, A bench study on lead removal from battery manufacturing wastewater by carbonate precipitation, *Water Res.*, 30 (1996) 3032–3036.
- [10] J.P. Chen, H. Yu, Lead removal from synthetic wastewater by crystallization in a fluidized-bed reactor, *J. Environ. Sci. Heal. A*, 35 (2000) 817–835.
- [11] C.S. Chen, Y.J. Shih, Y.H. Huang, Remediation of lead (Pb(II)) wastewater through recovery of lead carbonate in a fluidized-bed homogeneous crystallization (FBHC) system, *Chem/Eng. J.*, 279 (2015) 120–128.
- [12] R. Aldaco, A. Garea, A. Irabien, Calcium fluoride recovery from fluoride wastewater in a fluidized bed reactor, *Water Res.*, 41 (2007) 810–818.
- [13] R. Aldaco, A. Garea, A. Irabien, Particle growth kinetics of calcium fluoride in a fluidized bed reactor, *Chem. Eng. Sci.*, 62 (2007) 2958–2966.
- [14] C.P. Huang, J.R. Pan, M.S. Lee, S.M. Yen, Treatment of high-level arsenic-containing wastewater by fluidized bed crystallization process, *J. Chem. Technol. Biotechnol.*, 82 (2007) 289–294.
- [15] N. Boonrattanakij, M.C. Lu, J. Anotai, Iron crystallization in a fluidized-bed Fenton process, *Water Res.*, 45 (2011) 3255–3262.
- [16] C.C. Su, C.M. Chen, J. Anotai, M.C. Lu, Removal of monoethanolamine and phosphate from thin-film transistor liquid crystal display (TFT-LCD) wastewater by the fluidized bed Fenton process, *Chem. Eng. J.*, 222 (2013) 128–135.
- [17] C. Su, L. Dulfo, M. Dalida, M-C Lu, Magnesium phosphate crystallization in a fluidized-bed reactor: effects of pH, Mg:P molar ratio and seed. *Sep. Purif. Technol.*, 125 (2014) 90–96.
- [18] M.S. Rahaman, D.S. Mavinic, A. Meikleham, N. Ellis, Modeling phosphorus removal and recovery from anaerobic digester supernatant through struvite crystallization in a fluidized-bed reactor, *Water Res.*, 51 (2014) 1–10.
- [19] A.E. Nielsen, Electrolyte crystal growth kinetics, *J. Cryst. Growth*, 67 (1984) 278–288.
- [20] A.S. Myerson, *Handbook of Industrial Crystallization*, 2nd ed., Butterworth-Heinemann, 2002.
- [21] R. Aldaco, A. Garea, A. Irabien, Modeling of particle growth: application to water treatment in a fluidized bed reactor, *Chem. Eng. J.*, 134 (2007) 66–71.
- [22] M.I.H. Bhuiyan, D.S. Mavinic, R.D. Beckie, Nucleation and growth kinetics of struvite in a fluidized bed reactor, *J. Cryst. Growth*, 310 (2008) 1187–1194.
- [23] J.D. Hem, C.E. Roberson, Form and Stability of Aluminum Hydroxide Complexes in Dilute Solution, U.S. Geol. Survey Water-Supply Paper 1827-A, United States Government Printing Office, Washington, 1967, pp. 55.
- [24] W.Q. Cai, H.Q. Li, Y. Zhang, Influences of processing techniques of the  $H_2O_2$  precipitated pseudoboehmite on the structural and textural properties of  $\gamma-Al_2O_3$ , *Colloid Surf. A*, 295 (2007) 185–192.
- [25] E.A. El-Katatny, S.A. Halawy, M.A. Mohamed, M. Zaki, A novel synthesis of high-area alumina *via*  $H_2O_2$ -precipitated boehmite from sodium aluminate solutions, *J. Chem. Technol. Biotechnol.*, 72 (1998) 320–328.
- [26] Y.L. Xie, S.W. Bi, Y.H. Yang, Z. Wang, Research on structure of sodium aluminate solution in alumina production, *Nonferrous Metals*, 53 (2001) 59–61.
- [27] S. Marciano, N. Mugnier, P. Clerin, B. Cristol, P. Moulin, Nanofiltration of Bayer process solutions, *J. Membr. Sci.*, 281 (2006) 260–267.
- [28] G.C. Kennedy, Phase relations in the system  $Al_2O_3-H_2O$  at high temperatures and pressures, *Am. J. Sci.*, 247 (1959) 563–573.
- [29] K. Wefers, C. Misra, Oxides and Hydroxides of Aluminum, Alcoa Tech. Paper No. 19, Aluminum Company of America, Revised, 1987.
- [30] K.H. Gayer, L. Thompson, O.T. Zajicek, The solubility of aluminum hydroxide in acidic and basic media at 25°C, *Canadian J. Chem.*, 36 (1958) 1268–1271.
- [31] R.W. Smith, J.D. Hem, Effect of Aging of Aluminum Hydroxide Complexes in Dilute Solutions, Chemistry of Aluminum in Natural Water, United States Government Printing Office, Washington, 1972.
- [32] J. Chung, E. Jeong, J.W. Choi, S.T. Yun, S.K. Maeng, S.W. Hong, Factors affecting crystallization of copper sulfide in fed-batch fluidized bed reactor, *Hydrometallurgy*, 152 (2015) 107–112.
- [33] G.V. Franks, Y. Gan, Charging behavior at the alumina-water interface and implications for ceramic processing, *J. Am. Ceram. Soc.*, 90 (2007) 3373–3388.
- [34] D.A. Sverjensky, Zero-point-of-charge prediction from crystal chemistry and salvation theory, *Geochim. Cosmochim. Acta*, 58 (1994) 3123–3129.
- [35] C.Y. Tai, W.C. Chien, C.Y. Chen, Crystal growth kinetics of calcite in a dense fluidized bed crystallizer, *AIChE J.*, 45 (1999) 1605–1614.
- [36] J.M. Kim, S.M. Chang, J.H. Chang, W.S. Kim, Agglomeration of nickel/cobalt/ manganese hydroxide crystals in Couette-Taylor crystallizer, *Colloid. Surf. A*, 384 (2011) 3–39.
- [37] Y. Shimizu, I. Hirasawa, Effect of seeding on metal ion recovery from wastewater by reactive crystallization of metal carbonates, *Chem. Eng. Technol.*, 35 (2012) 1588–1592.